Phys. Status Solidi C **6**, No. S2, S557–S560 (2009) / **DOI** 10.1002/pssc.200880901

physica status solidi c
www.pss-c.com
current topics in solid state physics

Influence of strain and polarisation on electronic properties of a GaN/AlN quantum dot

Toby D. Young[*,1] **and Oliver Marquardt**[2]

[1] Instytut Podstawowych Prolemów Techniki Polska Academia Nauk, Świętokrzyska 21, 00-049 Warsaw, Poland
[2] Max-Planck-Institut für Eisenforschung, Max-Planck-Straße 1, 40237 Düsseldorf, Germany

Received 10 September 2008, revised 15 October 2008, accepted 21 October 2008
Published online 23 January 2009

PACS 68.35.bg, 68.35.Gy, 73.21.La, 77.65.Lyj, 78.66.Fd

* Corresponding author: e-mail tyoung@ippt.gov.pl, Phone: +48-22-8261281, Fax: +48-22-8269815

It is known that heterojunctions give rise to changes in the elastic and piezoelectric properties of a given semiconductor nanostructure. For practical applications it is decisive to understand the influence of these strain and piezoelectric fields on the electronic response of these systems, both as distinct and as coupled fields. In the present study, the confinement properties of the electron and hole wavefunctions are of interest. Therefore, a model based on a traditional envelope 8-band $\boldsymbol{k}\cdot\boldsymbol{p}$ Hamiltonian is implemented and used to explore a GaN/AlN quantum dot/matrix system.

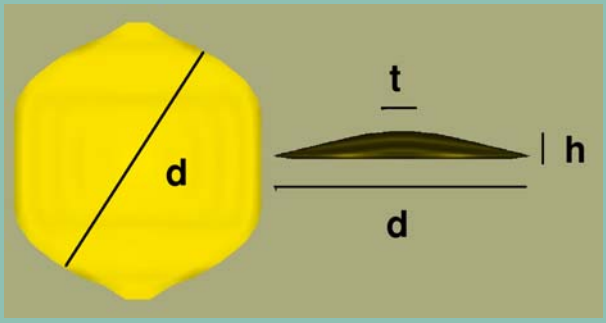

Profile of the buried hexagonal quantum dot: height $h = 4$ nm, diameter $d = 20$ nm and upper-truncation diameter $t = 4$ nm.

1 Introduction In recent years there has been a high interest in the growth as well as in the theoretical and experimental characterization of nitride-based semiconductor devices. The electronic and optical properties of wide band-gap type III-N heterostructures in particular have received considerable attention. Nanostructures, such as for example, quantum wells, wires, and dots, usually consist of two (or more) material types that have competing physical properties. In particular lattice mismatch, elastic properties, piezoelectric and pyroelectric effects, and the local space-group, play an important role in the emergent physical attributes of nanostructures.

The spontaneous polarisation arising in nanostructures with wurtzite crystal structure is known to lead to a spatial separation of electron and hole states and thus to reduce the effective oscillator strength between pairs inducing enhanced radiative lifetimes (see for example Ref. [1–3]). Having a practicable manipulation of these physical properties in mind, it is important to investigate the influence of strain and strain-induced piezoelectric fields on the electronic and optical response of these systems. In this work the effect of these two fields on the charge carrier wave functions and binding energies is investigated using a semi-classical model for cases in which they are considered as both distinct and as coexisting fields.

2 Background We have chosen to model a (wurtzite) hexagonal GaN/AlN quantum dot/matrix heterostructure (see also abstract figure) where size and shape are based on experimental observations of quantum dots by high resolution transmission electron microscopy [4]. The geometry of a hexagonal quantum dot is parameterised in Cartesian coordinates by three variables; the height h, the diameter d, and the upper-truncation t. Since the $\boldsymbol{k}\cdot\boldsymbol{p}$ for-

malism used in this work is a continuum approach, one needs to make sure that the physical properties are not dominated by effects related to the atomistic lattice, especially around the interfaces between dot and matrix material. Therefore a sufficiently large quantum dot was chosen. Periodic boundary conditions in each of the equivalent xyz-directions were applied and the matrix surrounding the quantum dot was determined to be large enough such that the dot does not interact with periodically repeated images of itself.

2.1 Model The 8-band $\boldsymbol{k}\cdot\boldsymbol{p}$ Hamiltonian matrix can be written as a sum of three parts [5,6]

$$H_{8\times8} = H_0 + H_{\text{strain}} + V_{\text{e}} \quad , \tag{1}$$

where H_0 describes band structure of the lowest conduction and the three highest valence bands around the Γ-point in the unstrained case. H_{strain} introduces the strain-dependent coupling and V_{e} is the electrostatic potential. The envelope wavefunctions of electron and hole states and their corresponding binding energies are determined from a diagonalisation of the Hamiltonian matrix $H_{8\times8}$.

2.2 Fields A precursor to the solution of the 8-band $\boldsymbol{k}\cdot\boldsymbol{p}$ Hamiltonian is thus to determine the strain and piezoelectric fields residing in the system. For this purpose an anisotropic non-linear theory of hyper-elasticity [7] was employed by utilising the so-called 'true' or 'Hencky' strain measure $\varepsilon = \log(u)$ (a logarithmic function of the displacement u). To take into account piezoelectric non-linearity we have adopted a model following Ref. [8], which assumes a strain dependency of the piezoelectric constants.

By assuming that there are no initial potential fields present in the system and that the quantum dot is charge free, the final state of the system is determined by the solution to the stress (σ) equilibrium equation,

$$\text{div}(\sigma) = 0 \quad . \tag{2}$$

An additional constraint is the equilibrium equation for the electrostatic displacement D

$$\text{div}(D) = 0 \quad , \tag{3}$$

where

$$D = \epsilon\nabla\phi + P_{\text{piezo}} + P_{\text{spont}} \quad , \tag{4}$$

containing contributions from piezoelectric (P_{piezo}) and spontaneous polarisation (P_{spont}). Following reference [9], we use a locally anisotropic dielectric constant ϵ. Due to the coupling of Eqn. (2) and (3) the piezoelectric field is determined by the strain present in the system whereas spontaneous polarisation is a property of wurtzite semiconductor materials. In this work a value of $P^{\text{GaN}}_{\text{spont}} = -0.029\,\text{C/m}^2$ and $P^{\text{AlN}}_{\text{spont}} = -0.081\,\text{C/m}^2$ were used respectively for wurtzite GaN and AlN; *cf.* Ref. [2].

2.3 Scheme Using these modelling tools, we investigate all possible combinations including strain and electrostatic fields in the $\boldsymbol{k}\cdot\boldsymbol{p}$ Hamiltonian (1), namely:

- (A) $H_{\text{strain}} = 0$ and $V_{\text{e}} = 0$, i.e. no strain and no electrostatic fields (a particle-in-a-box);
- (B) $H_{\text{strain}} \neq 0$, $V_{\text{e}} = 0$, i.e. non-zero strain field and no electrostatic field;
- (C) $H_{\text{strain}} = 0$, $V_{\text{e}} \neq 0$, i.e. no strain field and non-zero electrostatic field; and
- (D) $H_{\text{strain}} \neq 0$, $V_{\text{e}} \neq 0$, i.e. coupled strain and electrostatic fields.

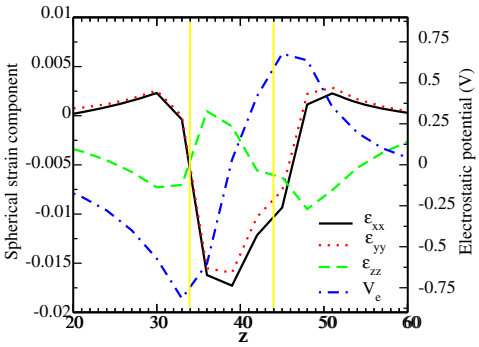

Figure 1 Spherical components of the strain field ε_{ii} through the centre of the quantum dot in the z-direction (see legend) .The dashed-dot line is the electrostatic potential V_{e}. Vertical bars denote the locations of the bottom and top surfaces of the quantum dot respectively.

3 Discussion The three so-called 'spherical' components of the strain field ε_{ii} derived from Eqn. (2) and the magnitude of the electrostatic field V_{e} obtained from Eqn. (3) are given in Fig. 1. The electrostatic field is found to be of the order of one volt and polarised in the z-direction (see also right-hand panel Fig. 2). The fields found here are in qualitative agreement with those of Ref. [2].

The binding energies of the first four electron (e_i) and hole states (h_i) in the cases (A-D) are listed in Table 1.

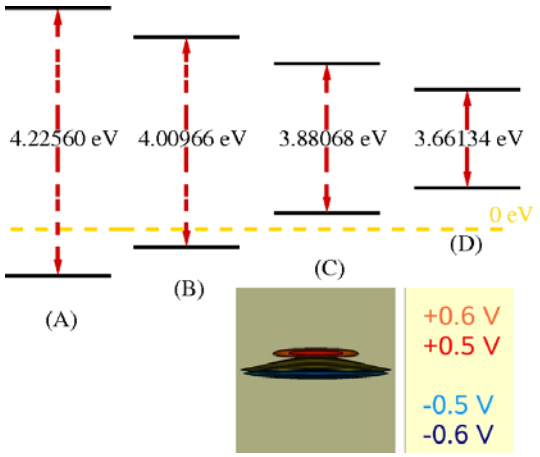

Figure 2 Shift of the transition energies between the lowest electron-hole pairs in each of the investigated four cases (A-D). On the right, the localisation of the electrostatic field in the quantum dot is sketched (cases (C-D) only).

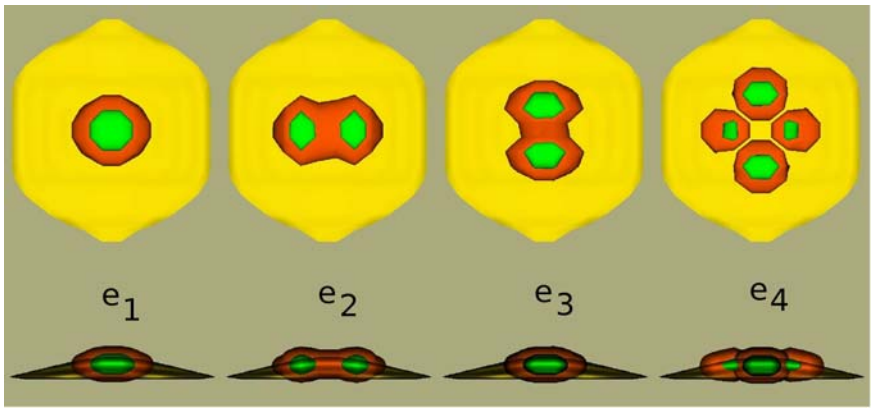

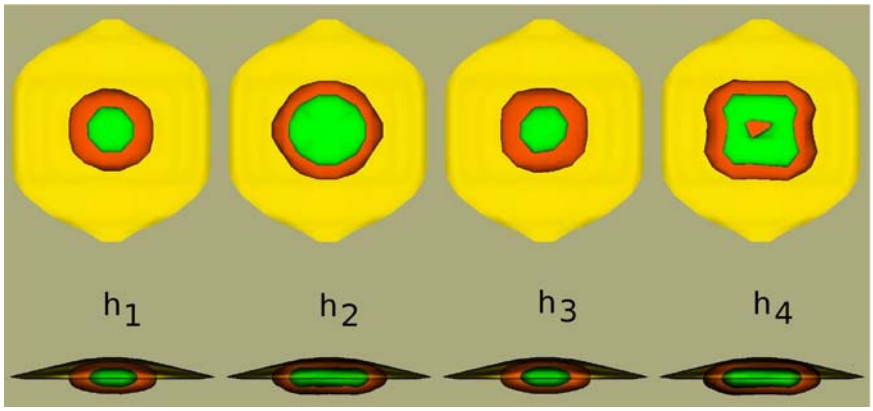

Figure 3 Iso-surface samples of the probability density of the four lowest-lying electron and hole envelope functions for case (D), where coupled strain and electrostatic fields have been taken into account (top panel: electron states, bottom panel: hole states).

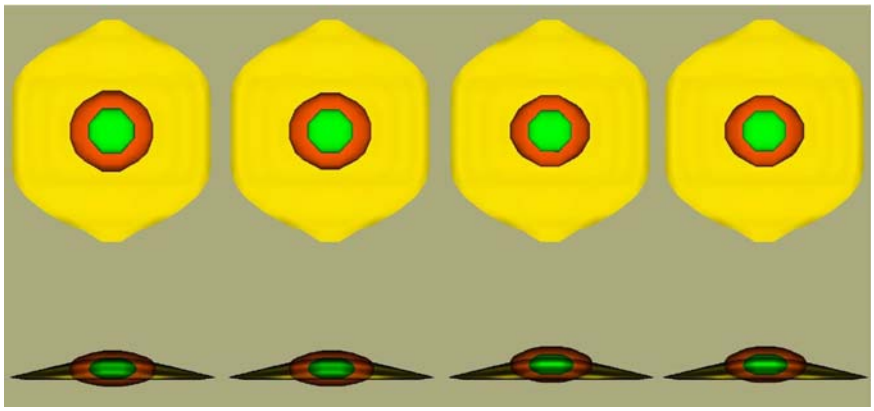

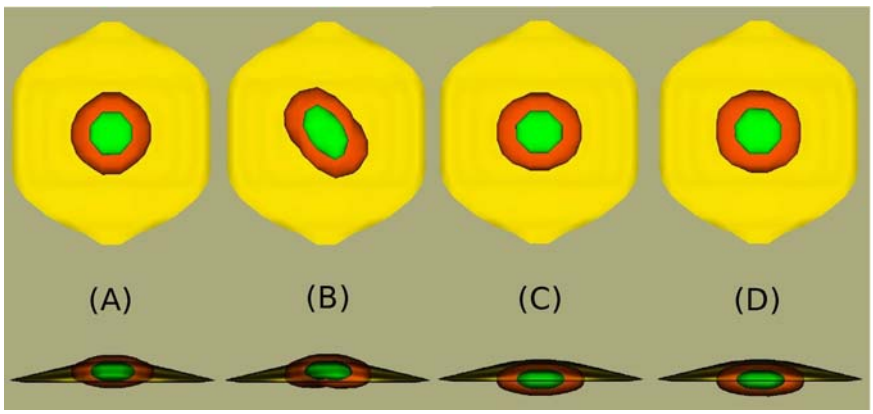

Figure 4 Same as in Fig. 3 but for the lowest-lying (ground-state) electron and hole probability density functions in the states (A-D).

Table 1 Energy of the first four electron-hole eigenstates obtained from diagonalisation of the 8-band $\boldsymbol{k}\cdot\boldsymbol{p}$-Hamiltonian in eVs. The vacuum state (0 eV) refers to the bulk GaN valence band offset.

State	(A)	(B)	(C)	(D)
e_4	4.24929	4.07042	4.25702	4.07934
e_3	4.13190	3.93549	4.11789	3.92056
e_2	4.12892	3.93434	4.11342	3.92014
e_1	4.01962	3.81173	3.97976	3.77341
h_1	-0.20256	-0.19793	0.09908	0.11207
h_2	-0.20675	-0.20889	0.08066	0.09653
h_3	-0.21734	-0.21194	0.07981	0.09187
h_4	-0.24096	-0.21821	0.06236	0.07803

The band energies $E_0 = E(e_1) - E(h_1)$, *ie.* the transition energy between the lowest-lying electron and lowest-lying hole state, is illustrated in Fig. 2. In the presence of a strain and/or polarisation field, there is a general trend of a negative shift in the band energy for electrons and a positive shift for the holes; indicating a reduction of the e_1-h_1 transition energy. It is clear from Fig. 2 that this indeed the case. It is interesting to note that the effect of polarisation (C) on this energy is approximately twice as high as that of strain (B). In particular, in the presence of the polarised electrostatic potential the hole states are shifted above the GaN band-offset (0 eV). We note, that the effect of screening of the internal potential due to the creation of excitons and/or charges on the surface of heterojunctions were not considered here. These effect are generally believed to increase the band-offset by a few meVs. To take into account these effects a self-consistent determination of the electric potential is desireable; typically, by employing a Schrödinger-Poisson self-consistent model [10, 11].

Figure 3 gives iso-surface samples of the probability density for the complete spectrum found from the 8-band $\boldsymbol{k}\cdot\boldsymbol{p}$ Hamiltonian where both strain and electrostatic fields are included. The results are in good agreement with Ref. [2] besides the energy difference between the first two hole states which results from the spin-orbit coupling (neglected in [2]). We may therefore infer the constitute parts of our model – the strain field and electrostatic potential *cf.* Eqn. (1) – are similarly in good agreement. The separation of the electron-hole states due to the polarisation of the electrostatic field is notable and comparable to that found in Ref. [2, 9], where here electrons are localised at the top and holes are localised at the bottom of the quantum dot. Additionally, we note an apparent change of the hole state shape in Fig. 4. The strained-only hole state (B) has an ellipsoidal probability density, while the hole ground state in case (D) - also strained - has an oblate spheroidal profile. This effect is due to the addition of polarisation in case (D), which causes the valence band offset to have a stronger localised minimum in the lower centre of the dot. This seems to lead to a stronger localisation there and therefore the ellipsoid shape of the state returns to its oblate spheroidal symmetry. This feature becomes only apparent by a comparison of distinct and coupled fields in quantum dot structures. We conclude that while the effect of polarisation has a stronger effect with respect to the *localisation* of the wavefunction in space, strain has a stronger influence on the *geometry* of the resultant wavefunction. However, the quantification of this phenomena needs further investigation.

4 Summary In this paper the strain and electrostatic fields in a buried GaN/AlN quantum dot/matrix were determined and the influence of these fields on the envelope electron and hole wavefunctions within an 8-band $\boldsymbol{k}\cdot\boldsymbol{p}$ model were investigated. It has been shown that the piezoelectric field influences:

1. The valence and conduction band offsets resulting in a smaller energy gap and the emitted wave length; and
2. The localisation of the charge carriers which leads to a reduced overlap of the corresponding wave functions which explains the small oscillator strength and the resulting long radiative decay time in wurtzite quantum dots.

Acknowledgements The authors would like to thank Dr. Tilmann Hickel for fruitful hints and discussion. This work was funded under the EC PARSEM project MRTN-CT-2004-005583.

References

[1] J. Simon, N. T. Pelekanos, C. Adelmann, E. Martinez-Guerrero, R. André, B. Daudin, Le Si Dang, and H. Mariette, Phys. Rev. B **68**, 035312 (2003).
[2] V. A. Fonoberov and A. A. Balandin, J. Appl. Phys. **94**(11), 7178 (2003).
[3] N. Baer, S. Schulz, P. Gartner, S. Schumacher, G. Czycholl, and F. Jahnke, Phys. Rev. B **76**, 075310 (2007).
[4] P. J. L. Rouviere, J. Simon, N. Pelekanos, B. Daudin, and G. Feuillet, Appl. Phys. Lett. **75**, 2632 (1999).
[5] S. L. Chuang and C. S. Chang, Phys. Rev. B **54**, 2491 (1996).
[6] J. Bhattacharyya and S. Ghosh, Phys. Status Solidi A **204**(11), 439 (2007).
[7] P. Dłużewski, G. Maciejewski, G. Jurczak, S. Kret, and J.-L. Laval, Comput. Mater. Sci. **29**, 379 (2004).
[8] K. Shimada, T. Sota, K. Suzuki, and H. Okumura, Jpn. J. Appl. Phys. **37**, L1421 (1998).
[9] A. S. Andreev and E. P. O'Reilly, Phys. Rev. B **62**, 15851 (2000).
[10] V. Ranjan, G. Allan, C. Priester, and C. Delerue, Phys. Rev. B **68**, 115305 (2003).
[11] S. Kalliakos, T. Bretagnon, P. Lefebvre, S. Juillaguet, T. Taliercio, T. Guillet, B. Gil, N. Grandjean, B. Damilano, A. Dussaigne, and J. Massies, Phys. Status Solidi B **241**, 2779 (2004).

